11142 *Inorg. Chem.* **2009**, *48*, 11142–11146
DOI: 10.1021/ic9015178

Inorganic Chemistry
Article

Luminescence Properties of Lanthanide and Transition Metal Ion-Doped Ba_2LaNbO_6: Detection of MnO_6^{8-} and CrO_6^{9-} Clusters

Peter A. Tanner*,† and Zaifa Pan†,‡

†*Department of Biology and Chemistry, City University of Hong Kong, Tat Chee Avenue, Kowloon, Hong Kong SAR, People's Republic of China, and* ‡*College of Chemical Engineering and Materials Science, Zhejiang University of Technology, Hangzhou, Zhejiang 310014, People's Republic of China*

Received July 30, 2009

The *as-prepared* double-perovskite Ba_2LaNbO_6 (space group $I2/m$ at ambient temperatures) exhibited an unexpected well-resolved red luminescence, which was found to arise from parts-per-million impurity of Mn^{4+}. The ions Mn^{4+} or Cr^{3+} doped into this host are situated at Nb^{5+} sites with slightly distorted octahedral symmetry, with the distortion greater for the case of greater charge mismatch. The Stokes luminescence spectra of the dopant ions comprise ν_3, ν_4, and ν_6 moiety mode vibronic origins, and the high vibrational frequency ratio ν_4/ν_3 signals the stiffness of the O−M−O (M = Mn, Cr) angle in the double perovskite. The site symmetry at the La^{3+} site of lanthanide ions doped into Ba_2LaNbO_6 comprises a 2-fold axis at most. All dopant ions exhibit concentration quenching in this lattice.

1. Introduction

The series of compounds Ba_2LnNbO_6 (Ln = lanthanide) was first reported by Brixner[1] to have a simple cubic perovskite structure with the exception of Ba_2LaNbO_6, which was reported as a tetragonally distorted perovskite. Complex oxides with perovskite-type structure are interesting new substrate materials of high-T_c superconductors[2,3] and microwave dielectric resonators.[4,5] In recent years, the structure and magnetic properties of the double perovskites with formula Ba_2LnNbO_6 have been reinvestigated.[6−8] The most recent, definitive studies utilized synchrotron X-ray and neutron powder diffraction methods[9,10] for the series Ba_2LnMO_6 (M = Ta, Nb). Nearly all systems deviate from the high-temperature $Fm\bar{3}m$ cubic double perovskite by phase transitions to space groups such as $R\bar{3}$, $I4/m$, and $I2/m$ or the formation of two phases. The Ln^{3+} and M^{5+} ions are arranged alternately in LnO_6^{9-} and NbO_6^{7-} moieties, respectively, in rock salt sublattices with the octahedra tilted around one of the principal axes. The crystal distortion from cubic symmetry increases with increasing difference between the ionic radii of Ln^{3+} and Nb^{5+}, i.e., for the larger lanthanide ions. In the case of the $I2/m$ space group, the site symmetry of both the Ln^{3+} and M^{5+} ions is C_{2h}. Paschoal and Diniz[11] have performed a computer modeling of the physical properties of Ba_2LnNbO_6 compounds.

The vibrational spectra of some niobium and tantalum perovskites are available,[12−15] and several researches have focused upon the optical properties of Ba_2LnNbO_6. Blasse et al.[16] employed room-temperature luminescence to investigate the site symmetry of Eu^{3+} in Ba_2GdNbO_6 and concluded that Eu^{3+} is situated at a site of octahedral symmetry. Conflicting reports of concentration quenching have been reported for this system,[17,18] and evidently Li^+ codoping increases the photoluminescence intensity.[18] Qi et al.[19] reported that the emission spectrum of Nd^{3+} in Ba_2NdNbO_6 is

*To whom correspondence should be addressed. E-mail: bhtan@cityu.edu.hk.

(1) Brixner, H. *J. Inorg. Nucl. Chem.* **1960**, *15*, 352.
(2) Kurian, J.; Nair, K. V. O.; Sajith, P. K.; Koshy, J. *Appl. Supercond.* **1998**, *6*, 259.
(3) Nair, S. U. K.; Warriar, P. R. S.; Koshy, J. *J. Mater. Sci.* **2003**, *38*, 481.
(4) Khalam, L. A.; Sreemoolanathan, H.; Ratheesh, R.; Mohanan, P.; Sebastaian, M. T. *Mater. Sci. Eng., B* **2004**, *107*, 264.
(5) Korchagina, S. K.; Shevchuk, Yu. A. *Inorg. Mater.* **2006**, *42*, 64.
(6) Henmi, K.; Hinatsu, Y.; Masaki, N. M. *J. Solid State Chem.* **1999**, *148*, 353.
(7) Fu, W. T.; Iido, D. J. W. *J. Solid State Chem.* **2006**, *179*, 1022.
(8) Kurian, J.; Pai, S. P.; James, J.; Koshy, J. *J. Mater. Sci.: Mater. Electron.* **2001**, *12*, 173.
(9) Saines, P. J.; Spencer, J. R.; Kennedy, B. J.; Avdeev, M. *J. Solid State Chem.* **2007**, *180*, 2991.
(10) Saines, P. J.; Spencer, J. R.; Kennedy, B. J.; Kubota, Y.; Minakata, C.; Hano, H.; Kato, K.; Takata, M. *J. Solid State Chem.* **2007**, *180*, 3001.
(11) Paschoal, C. W. A.; Diniz, E. M. *J. Phys.: Condens. Matter* **2009**, *21*, 075901.
(12) Blasse, G.; van Tol, F. *Solid State Commun.* **1995**, *95*, 465.
(13) Dias, A.; Khalam, L. A.; Sebastian, M. T.; Paschoal, C. W. A.; Moreira, R. L. *Chem. Mater.* **2006**, *18*, 214.
(14) Dias, A.; Khalam, L. A.; Sebastian, M. T.; Moreira, R. L. *J. Solid State Chem.* **2007**, *180*, 2143.
(15) Lavat, A. E.; Baran, E. J. *Vibr. Spectrosc.* **2003**, *32*, 167.
(16) Blasse, G.; Bril, A.; Nieuwpoort, W. C. *J. Phys. Chem. Solids* **1966**, *27*, 1587.
(17) Xiao, X. Z.; Yan, B. *J. Alloys Compd.* **2007**, *433*, 246.
(18) Yu, C. C.; Liu, X. M.; Yu, M.; Lin, C. K.; Li, C. X.; Wang, H.; Lin, J. *J. Solid State Chem.* **2007**, *180*, 3058.
(19) Qi, X.; Gallagher, H. G.; Han, T. P. J. *Chem. Phys. Lett.* **1997**, *264*, 623.

 Published on Web 10/19/2009

broadened by crystal disorder. The lifetime of the $Nd^{3+4}F_{3/2}$ state in the Ba_2LaNbO_6 host exhibits pronounced concentration quenching.[20] More generally, the electronic absorption[21] and luminescence spectra[12,22−24] of the d^0 system Nb^{5+} have been the subject of many reports. The band gap of many NbO_6^{7-} systems lies in the range from 3.6 to 4.1 eV.[21] As Srivastava et al. have commented,[25] the excited state is expected to be delocalized in a structure that offers three-dimensional coupling of the d^0 metal ion polyhedra through corner sharing, when the $M^{n+}-O^{2-}-M^{n+}$ angle approaches 180°. Thus, the emission of Nb^{5+} comprises a broad feature between 350 and 700 nm, with a maximum between 440 and 575 nm, which has a Stokes shift of 9000−15000 cm^{-1}.

It was therefore surprising that we observed a structured emission band in the red spectral region for *neat* Ba_2LaNbO_6, which gave well-resolved individual features upon cooling to 10 K, as is subsequently described. The initial purpose of the present work was therefore to investigate the origin of this emission, and in doing so, we doped lanthanide or transition-metal ions into this host and studied their luminescence properties. Some insights concerning their coordination geometries and site occupations have been forthcoming from these results.

2. Experiment

The neat or doped Ba_2LaNbO_6 samples were prepared by a standard solid-state reaction method from the starting materials of $BaCO_3$ (Aldrich, 99.999%), La_2O_3 (Sigma-Aldrich, 99.999%), and Nb_2O_5 (Strem, 99.999%) in stoichiometric amounts and the dopants of Eu_2O_3, Cr_2O_3 (Sigma-Aldrich, 99.9%), or $Mn(CH_3COO)_2$ (Aldrich, 99%). The dopant ion concentrations were nominally 0.1 atom % for Eu^{3+} and Mn^{2+} and 0.035, 0.080, and 1.0 atom % for Cr^{3+}. A $Ba_2LaTaO_6:Nb^{5+}$ (1 atom %) sample was also prepared with Nb_2O_5 as the dopant, using Ta_2O_5 (Strem, 99.9%) as the starting material.

Normally, the appropriate mixture was ground, placed in a ceramic crucible, and prefired in air at 1000 °C for 12 h to decompose $BaCO_3$. The products were then reground, put into a platinum crucible, and sintered at 1200 °C for 20 h and then at 1300 and 1400 °C for 20 h in each step.

Powder X-ray diffraction patterns were obtained on a Siemens D500 X-ray diffractometer using Cu Kα radiation (λ = 1.54 Å) at 40 kV and 30 mA with a scanning rate of 0.05° s^{-1} in the 2θ range of 20−80°. FT-Raman spectra were recorded by a Perkin-Elmer 2000 spectrometer and FT-IR spectra by a Nicolet Avatar 360 instrument.

Room-temperature excitation and emission spectra (resolution ∼3 nm) were recorded by a Jobin-Yvon Fluoromax-3 spectrofluorometer. Luminescence spectra were recorded at higher resolution (∼0.2 nm) using the third harmonic of a Surelite Continuum Nd:YAG pulsed laser to pump a Panther optical parametric oscillator. The emission was collected at 90° by an Acton 0.5 m monochromator and detected by a back-illuminated SpectruMM CCD detector. The samples were housed in an Oxford Instruments closed-cycle cryostat.

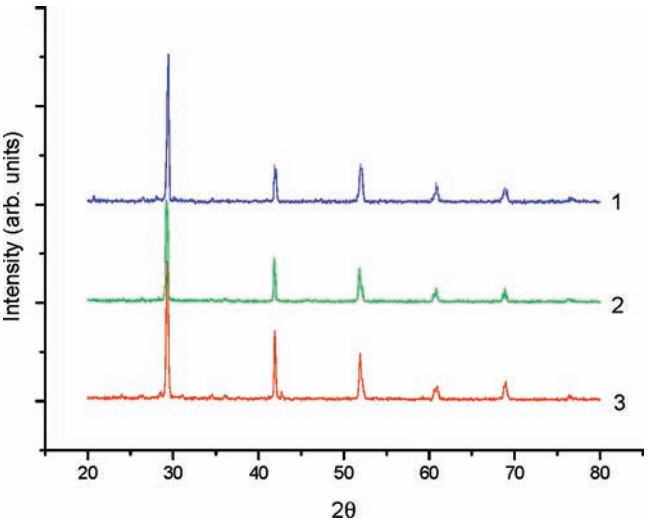

Figure 1. Powder X-ray diffraction patterns of (1) $Ba_2LaTaO_6:Nb^{5+}$ (1 atom %), (2) $Ba_2LaNbO_6:Pr^{3+}$ (0.1 atom %), and (3) neat Ba_2LaNbO_6.

Emission lifetimes were measured by a Tektronix TDS5054B digital phosphor oscilloscope with a Nd:YAG pulsed laser as the excitation source. A photodiode was utilized to record the laser trigger reference.

3. Results and Discussion

3.1. Powder X-ray Diffraction Patterns. Powder X-ray diffraction patterns of $Ba_2LaTaO_6:Nb^{5+}$ (1%), $Ba_2LaNbO_6:Pr^{3+}$ (0.1%), and neat Ba_2LaNbO_6 samples at room temperature are shown in Figure 1. All of the patterns are dominated by lines strongly resembling the primitive cubic perovskite, but many lines are clearly split, indicating that the crystal symmetries are lower than the cubic ones. The powder patterns are in agreement with those presented by Fu and Iido.[7]

3.2. Vibrational Spectra. Although the vibrational spectra of some perovskite oxides have been recorded, no detailed assignments and calculations of the frequencies are available. The FT-IR spectra of neat Ba_2LaNbO_6 and Ba_2LaNbO_6:Pr (0.1%) are similar (Figure S1 in the Supporting Information) and comprise a broad feature between 400 and 900 cm^{-1}, with a maximum at 507 cm^{-1} (attributed to the Nb−O antisymmetric stretching mode), upon which three shoulders are resolved at 447, 623, and 789 cm^{-1}. Lavat and Baran[15] have associated the intense, broad FT-IR band of Ba_2SmNbO_6 at 534 cm^{-1} with Nb−O stretching, whereas a lower-energy band at 337 cm^{-1} was associated with Sm−O stretching. The Raman spectra of perovskite oxides generally comprise three groups of bands between 350 and 1000 cm^{-1}.[14,26] Our FT-Raman spectrum of Ba_2LaNbO_6 exhibits bands (in cm^{-1}) in this region at 366 (medium), 381 (medium), 503 (weak), and 797 (weak). The highest-energy bands are associated with Nb−O symmetric stretching (ν_1 and ν_2) and the 366 and 381 cm^{-1} bands with O−Nb−O bending (ν_5), where the ν_i labels refer to parent octahedral modes. In addition, stronger bands at 1002, 1040, and 1367 cm^{-1} are observed in this 1064.2 nm excited Raman spectrum (Figure S1 in the Supporting Information) and are discussed in the

(20) Merchandt, P.; Grannec, J.; Chaminade, J. P. *Mater. Res. Bull.* **1980**, *15*, 1113.
(21) Eng, H. W.; Barnes, P. W.; Auer, B. M.; Woodward, P. M. *J. Solid State Chem.* **2003**, *175*, 94.
(22) Hsiao, Y.-J.; Liu, C.-W.; Dai, B.-T.; Chang, Y.-H. *J. Alloys Compd.* **2009**, *475*, 698.
(23) Blasse, G.; Brixner, L. H. *Mater. Res. Bull.* **1989**, *24*, 363.
(24) Blasse, G.; Dirksen, G. J.; Crosnier, M. P.; Piffard, Y. *J. Alloys Compd.* **1992**, *189*, 259.
(25) Srivastava, A. M.; Ackerman, J. F.; Beers, W. W. *J. Solid State Chem.* **1997**, *134*, 187.
(26) Corsmit, A. F.; Hoefdraad, H. E.; Blasse, G. *J. Inorg. Nucl. Chem.* **1972**, *34*, 3401.

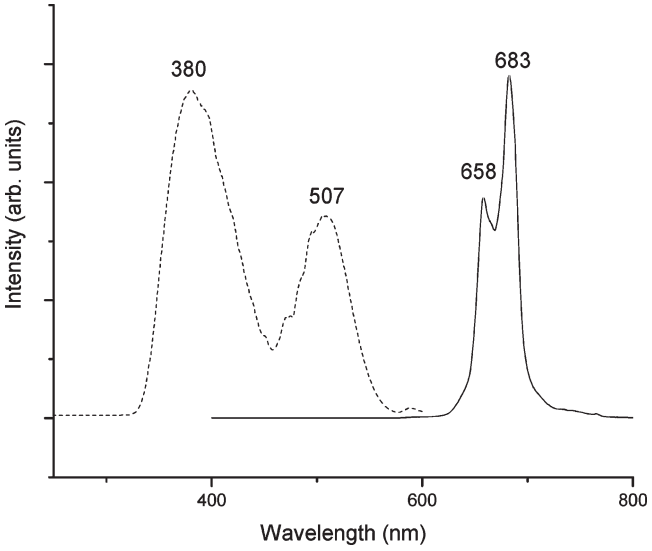

Figure 2. Room-temperature excitation (dotted line) and emission (full line) spectra of an as-prepared Ba_2LaNbO_6 sample: λ_{em} = 683 nm; λ_{exc} = 380 nm. The wavelengths of the bands are in nanometers.

Conclusions section. The splitting of parent octahedral modes is expected from the descent from the octahedral symmetry of the NbO_6 moiety.

3.3. Photoluminescence of As-Prepared Ba_2LaNbO_6. Figure 2 shows the low-resolution 360 nm excited emission spectrum of *as-prepared* Ba_2LaNbO_6 in the visible spectral region at room temperature. Two features are observed in the red spectral region, at 658 and 683 nm. The excitation spectrum of each feature is the same, with broad bands at 380 and 507 nm. The nature of the luminescent center was investigated by intentionally doping various ions into Ba_2LaNbO_6 and recording the emission and excitation spectra. It was determined that the spectra were identical when doping a small amount of Mn^{2+}, but evidently this ion is oxidized to Mn^{4+} because the spectra of these two ions are readily distinguished.[27−32] The bands in the excitation spectra correspond to the $^4A_2 \rightarrow {}^4T_2$ and $^4A_2 \rightarrow {}^4T_1$ transitions, in order of increasing energy, whereas the red emission corresponds to $^2E \rightarrow {}^4A_2$. The emission was fitted with monoexponential lifetimes of 0.77 ± 0.02 ms at 30 K, 0.71 ms at 120 K, and 0.63 ms at 250 K. These values are comparable to the lifetimes of Mn^{4+} at various sites in $YAlO_3$, which lie between 0.41 and 5.4 ms at 77 K.[29] Three strong Stokes bands are partially resolved at room temperature at 678.2, 680.5, and 684.0 nm (in Figure 3, at 295 K: 14 746, 14 695, and 14 619 cm^{-1}). These features do not correspond to Mn^{4+} ions at three different sites, as for Mn^{4+} in Ca- or Mg-substituted $Gd_3Ga_5O_{12}$.[30] The temperature dependence of the spectrum was studied under high resolution (Figure 3: 295−10 K), and it became evident that the room-temperature bands of Figure 2 at

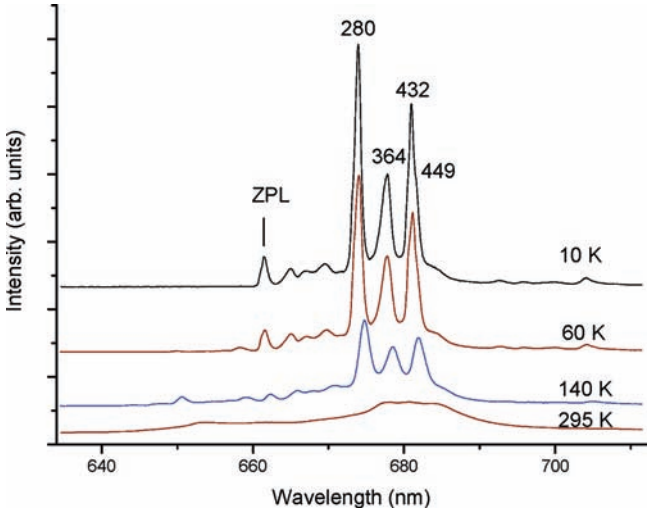

Figure 3. Temperature dependence of the 355 nm excited emission spectrum of the Mn^{4+} impurity in Ba_2LaNbO_6 between 634 and 712 nm from 295 to 10 K. The plots have been shifted vertically for clarity, but the relative intensities are preserved. The zero phonon line (ZPL) and displacements (in cm^{-1}) of the vibrational structure ν_6, ν_4, and ν_3 are marked.

658 and 683 nm corresponded to unresolved anti-Stokes and Stokes vibronic components, respectively. The relative intensities of bands in the low-temperature spectra were independent of the laser excitation line employed (Figure S2 in the Supporting Information), showing that the emission occurs from one species. From the very weak zero phonon line at room temperature and its relatively low intensity at lower temperatures, it is clear that the luminescence center is situated at a site with a slight distortion from inversion symmetry. The zero phonon (R) line exhibits a blue shift with decreasing temperature (Figure S3 in the Supporting Information), which is the reverse of that for $YAlO_3:Mn^{4+}$, and signals the reverse difference in zero-point energies of the ground $^4A_2$ and ^2E excited states. A splitting of the R lines at 15 116 and 15 126 cm^{-1} by ~10 cm^{-1} is evident below ~60 K (Figure S3 in the Supporting Information). The lower-energy feature is more intense, as expected from the Boltzmann equilibrium. The six-coordination ionic radii of Nb^{5+} and La^{3+} are 64 and 103.2 pm, respectively, whereas the Ba^{2+}(XII) radius is 161 pm.[33] Clearly, from the sharp spectral lines in emission, it is evident that the Mn^{4+} ion substitutes at a regular crystallographic site. It is therefore most likely that the Mn^{4+} ion, with an ionic radius Mn^{4+}(VI) of 53 pm, substitutes at the Nb^{5+} site.[33] The distortion from octahedral symmetry is expected for substitution at the C_{2h} site, as well as from the lattice arrangement for charge compensation. From the similarity of the three strong Stokes bands with analogous features in perfectly octahedral MnF_6^{2-},[31] these bands can be assigned to the ungerade moiety modes ν_6 (280 cm^{-1}), ν_4 (364 cm^{-1}), and ν_3 (432 and 449 cm^{-1}) of MnO_6^{8-}. An objection to this assignment could be raised from the high ratio of the ν_4/ν_3 frequencies (0.83), which compares with those for other metal oxides (~0.7) and fluorides (~0.5).[34]

(27) Yu, C. F.; Lin, P. *J. Appl. Phys.* **1996**, *79*, 7191.
(28) Hsu, K.-H.; Yang, M.-R.; Chen, K.-S. *J. Mater. Sci.* **1998**, *9*, 283.
(29) Zhydachevskii, Y.; Galanciak, D.; Kobyakov, S.; Berkowski, M.; Kamińska, A.; Suchocki, A.; Zakharko, Y.; Durygin, A. *J. Phys.: Condens. Matter* **2006**, *18*, 11385.
(30) Noginov, M. A.; Loutts, G. B. *J. Opt. Soc. Am. B* **1999**, *16*, 3.
(31) Yeakel, W. C.; Schwartz, R. W.; Brittain, H. G.; Slater, J. L.; Schatz, P. N. *Mol. Phys.* **1976**, *32*, 1751.
(32) Brenier, A.; Suchocki, A.; Pedrini, C.; Boulon, G.; Madej, C. *Phys. Rev. B* **1992**, *46*, 3219.
(33) Shannon, R. D. *Acta Crystallogr., Sect. A* **1972**, *32*, 751. Available at http://abulafia.mt.ic.ac.uk/shannon/ptable.php.
(34) Nakamoto, K. *Infrared and Raman Spectra of Coordination Compounds*; 5th ed.; Wiley-Interscience: New York, 1997; Section II.

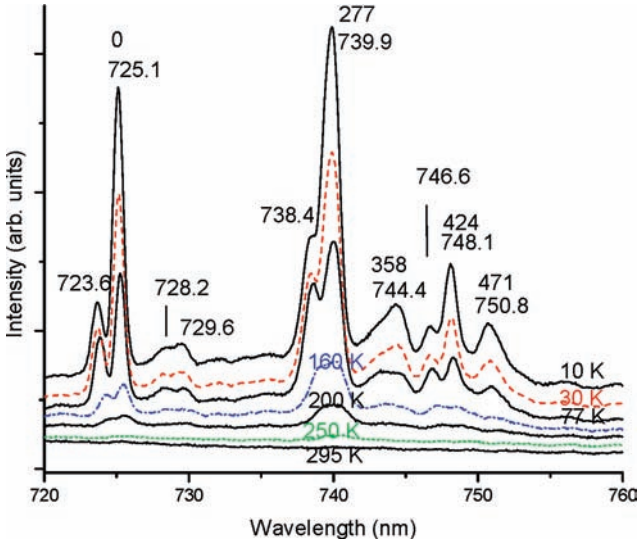

Figure 4. Temperature evolution of the emission of $Ba_2LaNbO_6:Cr^{3+}$ (0.08 atom %) excited at 355 nm from 295 to 10 K, as indicated. The wavelengths of bands are in nanometers, and above these are given the displacements, in cm^{-1}, of the ν_3, ν_4, and ν_6 vibronic structures from the R_1 zero phonon line (0).

Progressions are observed upon each vibronic origin in modes of 399 and 466 cm^{-1}, which correspond to ν_2 and ν_1.

In order to investigate further the Mn^{4+} contamination, a sample of $Ba_2LaTaO_6:Nb^{5+}$ (1 atom %) was prepared. The emission spectrum was considerably weaker in intensity (Figure S4 in the Supporting Information), showing conclusively that the origin of the manganese contamination was from Nb_2O_5. The stronger R zero phonon line exhibited a blue shift of 14 cm^{-1}, but otherwise the spectrum was very similar. The derived energies of ν_6 and ν_3 were very similar to those in Ba_2LaNbO_6, but ν_4 was ~10 cm^{-1} lower. The similarity in vibrational energies is expected because the ionic radii of Nb^{5+}(VI) and Ta^{5+}(VI) are the same so that the site occupied by Mn^{4+} is similar.

3.4. Photoluminescence of $Ba_2LaNbO_6:Cr^{3+}$. Upon doping Cr^{3+} at parts-per-million levels in Ba_2LaNbO_6, an additional group of bands is observed at low temperatures to a low energy of the Mn^{4+} emission, between 725 and 740 nm, which corresponds to the $^2E \rightarrow {}^4A_2$ 3d intrashell transition of Cr^{3+}. The temperature-dependent quenching of the Cr^{3+} emission, using 355 nm excitation, is shown in Figures 4 and S5 in the Supporting Information. As Srivastava et al. have mentioned,[25] the low quenching temperature arises in types of systems where three-dimensional coupling via M^{n+}−ligand−M^{n+} coupling occurs via corner sharing, so that energy migration to trap centers occurs. Concentration quenching also occurs for $Ba_2LaNbO_6:Cr^{3+}$ (Figure S6 in the Supporting Information), and quenching in this host has been interpreted as being due to dipole−dipole interactions between ions and/or due to exchange couplings.[20]

Analysis of the low-temperature spectrum (Figure 4), together with the consideration of anti-Stokes bands (not shown), confirms that the two bands at 723.6 and 725.1 nm correspond to the Cr^{3+} R_2 and R_1 lines, respectively. The major Stokes vibronic structure based upon these zero phonon lines is assigned to ν_6, ν_4, and ν_3 modes (in cm^{-1}) at 277, 358, and 448 (mean), respectively. Although for Cr^{3+} ions doped into low-symmetry hosts the R-line sideband structure is more representative of the host phonon density of states, these features can be assigned to octahedral moiety modes on the basis that the derived energies are very similar to those for Mn^{4+}. Again, the frequency ratio ν_4/ν_3 is high (0.8), especially when compared to the corresponding frequency ratio in $Cr(H_2O)_6^{3+}$ (0.59). However, the difference is readily understood from the rigid linearity restriction in the linear O−Cr−O angle in the La−O−Cr−O−La chain, which is not present in the aqua complex. The ionic radius of Cr^{3+}(VI) (61.5 pm) is appropriate for substitution at the Nb^{5+} site, but the deviation from the octahedral symmetry is expected both from substitution at the C_{2h} site and from the larger charge imbalance than for the case of Mn^{4+}. This is exemplified by not only the zero phonon line splitting (28 cm^{-1}) but also the splitting resolved for ν_3. The R_1 energy (13 791 cm^{-1}) is considerably lower than that for Cr^{3+} at the more compact octahedral site in α-Al_2O_3 (14 420 cm^{-1}), although the R_1-R_2 splitting is similar. The decay time measured of the R-line emission exhibited double-exponential behavior at 30 K, indicating population from Mn^{4+} and a longer decay lifetime of 4.2 ms for Cr^{3+} emission.

3.5. Luminescence of Lanthanide Ions in Ba_2LaNbO_6. The lanthanide ion Eu^{3+} is a useful spectroscopic probe of its environment due to the selection rules for electric dipole and magnetic dipole transitions. Blasse et al.[16] reported that the room-temperature emission spectrum of Eu^{3+}-activated Ba_2GdNbO_6 consists of a sharp line at 595 nm ($^5D_0 \rightarrow {}^7F_1$) and some weak and broad lines in the region 610−630 nm ($^5D_0 \rightarrow {}^7F_2$), as a consequence of the O_h site symmetry. An analogous interpretation was made from the spectra of $Ba_2GdTaO_6:Ce^{3+}$.[35] A simulation of the spectral embedded EuO_6^{9-} cluster in this host lattice gave poor agreement with experiment.[36] Other reports of the luminescence of $Ba_2LaNbO_6:Eu^{3+}$[17] and $Ba_2GdNbO_6:Eu^{3+}$[18] have been recorded at low resolution so that spectral features are not resolved. Although Ba_2GdNbO_6[16] and Ba_2LaNbO_6[8] were at one time considered to crystallize in the $Fm\bar{3}m$ system, more sensitive investigations have shown the respective space groups to be tetragonal $I4/m$[7] and monoclinic $I2/m$,[7] respectively, at ambient temperatures. The site symmetries of Eu^{3+} in these host crystals are therefore C_{4h} and C_{2h}, respectively. The room-temperature and 10 K emission spectra of Eu^{3+} in Ba_2LaNbO_6 are shown in Figure 5, with the temperature dependence illustrated in Figure S7 in the Supporting Information. The appearance of one peak for the $^5D_0 \rightarrow {}^7F_0$ transition, as well as three strong bands for $^5D_0 \rightarrow {}^7F_1$, shows that Eu^{3+} occupies only one crystallographic site, there is no inversion center, and the highest symmetry axis for the Eu^{3+} site is 2-fold. Weaker bands, which decorate the $^5D_0 \rightarrow {}^7F_1$ transition, correspond to phonon modes (in cm^{-1}) at 203, 349, 464, 531, and 689. The forced dipole transition $^5D_0 \rightarrow {}^7F_2$ is intense and comprises two bands at most. From the comparison of ionic radii, the Eu^{3+} ion (94.7 pm) is situated at the La^{3+} (103.2 pm) site.

(35) Slack, G. A.; Dole, S. L.; Tsoukala, V.; Nolas, G. S. *J. Opt. Soc. Am. B* **1994**, *11*, 961.
(36) Visser, O.; Visscher, L.; Aerts, P. J. C.; Nieuwpoort, W. C. *J. Chem. Phys.* **1992**, *96*, 2910.

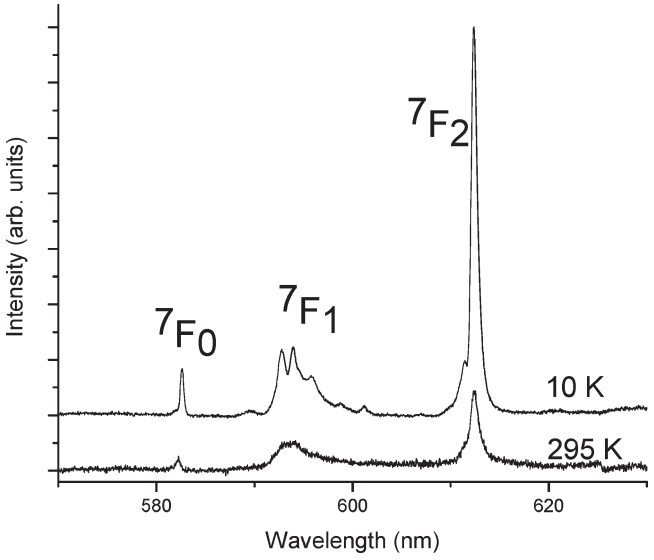

Figure 5. 355 nm excited emission spectrum of $Ba_2LaNbO_6:Eu^{3+}$ (0.1%) at room temperature and 10 K, between 570 and 630 nm.

4. Conclusions

The luminescence of Nb^{5+} is characterized by a very broad band in the visible spectral region, such as, for example, in $Ba_5Nb_4O_{15}$.[25] Thus, the well-resolved red emission from the as-prepared material Ba_2LaNbO_6 has instead been attributed to trace impurities of manganese in the double-perovskite host. Manganese exists in a wide range of oxidation states. Manganese(II) ($3d^5$) is octahedrally coordinated in $Mn(H_2O)_6^{2+}$ and in the mineral K_4MnCl_6. The electronic absorption spectra of these compounds are similar[39,40] but very different from the excitation spectrum of the manganese impurity in Ba_2LaNbO_6. The similarity of the excitation spectrum herein with that of Mn^{4+} compounds,[27−31] in particular that of $Gd_3Ga_5O_{12}:Mn^{4+}$,[32] clearly shows that Mn(IV) ($3d^3$), and not the precursor ion Mn(II), has substituted into the double perovskite. Although the oxide ion is stronger than fluoride in the spectrochemical series, the insensitivity of the $^2E-{}^4A_2$ energy separation to Dq/B in the Tanabe−Sugarno energy diagram leads to a fairly similar transition energy for the octahedral MnF_6^{2-} [31] and MnO_6^{8-} ions, at ∼16 040 and ∼15 120 cm^{-1}, respectively. Also, because the variation of the energy separation is flat with respect to Dq/B, the spin-forbidden transition $^2E-{}^4A_2$ gives sharp spectral features. Stokes and anti-Stokes vibronic structures form a mirror image from the zero phonon line. In fact, the low-temperature emission spectrum of $Ba_2LaNbO_6:Mn^{4+}$ strongly resembles that of the MnF_6^{4-} moiety in cubic host lattices.[31] Thus, the deduction of the site symmetry of Mn^{4+} in the double perovskite can be made from this similarity.

When lanthanide ions are diluted into Ba_2LaNbO_6, they do not occupy the Nb^{5+} site but rather prefer to substitute at the La^{3+} site. The site symmetry is found to comprise a 2-fold axis or plane of symmetry at most. The emission spectra exhibit marked concentration quenching, which has been attributed to excitation migration terminating at killer trap sites. Some other double-perovskite oxide hosts, such as Ba_2YbTaO_6 and Ba_2YNbO_6, are reported to crystallize in the $Fm\bar{3}m$ space group. An investigation of the crystal-field levels of some lanthanide ions in these oxide hosts would be useful for comparison with the abundant data available for octahedral fluoro and chloro complexes.

Finally, the nature of the luminescent impurity observed at ∼1000 cm^{-1} in the FT-Raman spectrum of neat Ba_2LaNbO_6 needs to be clarified. We have previously noted[43] that lanthanide ions (such as Ho^{3+}, Nd^{3+}, Yb^{3+}, and Er^{3+}) are capable of such interference, but because other emission bands are not observed under appropriate excitation wavelengths, this IR luminescence is not due to lanthanide ions. A search of the spectra of transition-metal ions shows that the luminescence is most likely due to Mn^{5+}. IR luminescence from this ion, with the $3d^2$ electronic configuration, has previously been observed from the $^3T_2 \rightarrow {}^3A_2$ transition in the region of 1.1−1.4 μm in oxide hosts.[44−46] No other visible or IR emission is expected from this species. In the present case, the emission bands are also located in this region. It is not possible to make more detailed assignments from the room-temperature spectrum. The presence of Mn^{5+} is not unexpected when Mn^{4+} has been shown to be present as an impurity in neat Ba_2LaNbO_6, but the much smaller ion Mn^{5+} (ionic radius 330 pm) is stabilized in the tetraoxo coordination.

Acknowledgment. Financial support for this work from the Hong Kong Research Grants Council General Research Fund Grant CityU 102607 is gratefully acknowledged. This work was also supported by the National Science Foundation of China under Grant 10804099.

Supporting Information Available: FT-IR, FT-Raman, and emission spectra and plots of temperature and concentration dependence. This material is available free of charge via the Internet at http://pubs.acs.org.

(37) Jia, G.; Tanner, P. A.; Cheng, B.-M. *Chem. Phys. Lett.* **2009**, *474*, 97.
(38) Boutinaud, P.; Cavalli, E.; Bettinelli, M. *J. Phys.: Condens. Matter* **2007**, *19*, 386230.
(39) Miessler, G. L.; Tarr, D. A. *Inorganic Chemistry*; Prentice-Hall: Englewood Cliffs, NJ, 1991; p 325.
(40) Foster, J. J.; Gill, N. S. *J. Chem. Soc. A* **1968**, 2625.
(41) Jouini, A.; Yoshikawa, A.; Fukuda, T.; Boulon, G. *J. Cryst. Growth* **2006**, *293*, 517.
(42) Kruth, A.; Guth, U.; West, A. R. *J. Mater. Chem.* **1999**, *9*, 1579.
(43) Tanner, P. A.; Mak, C. S. K.; Siu, G. G. *Appl. Spectrosc.* **2002**, *56*, 670.
(44) Milstein, J. B.; Ackerman, J.; Holt, S. L.; McGarvey, B. R. *Inorg. Chem.* **1972**, *11*, 1178.
(45) Capobianco, J. A.; Cormier, G.; Moncorgé, R.; Manaa, H.; Bettinelli, M. *Appl. Phys. Lett.* **1992**, *60*, 163.
(46) Buijsse, B.; Schmidt, J.; Chan, I. Y.; Singel, D. J. *Phys. Rev. B* **1995**, *51*, 6215.